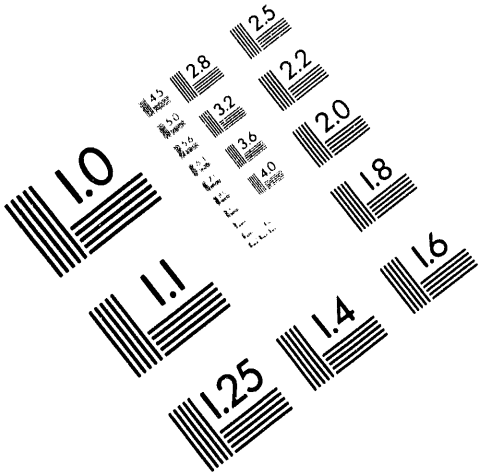

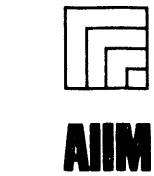

Association for Information and Image Management

1100 Wayne Avenue, Suite 1100
Silver Spring, Maryland 20910

301/587-8202

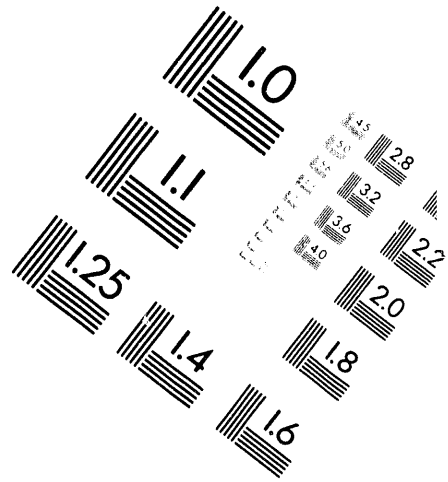

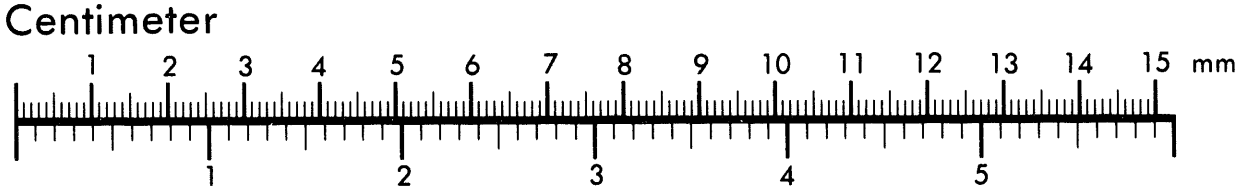

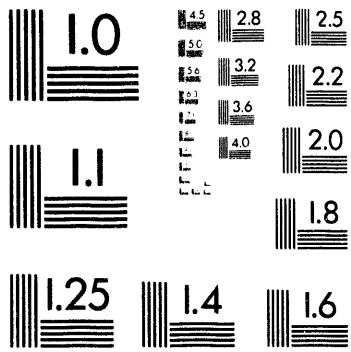

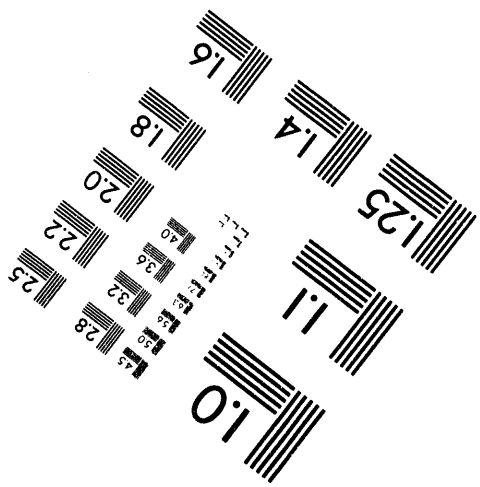

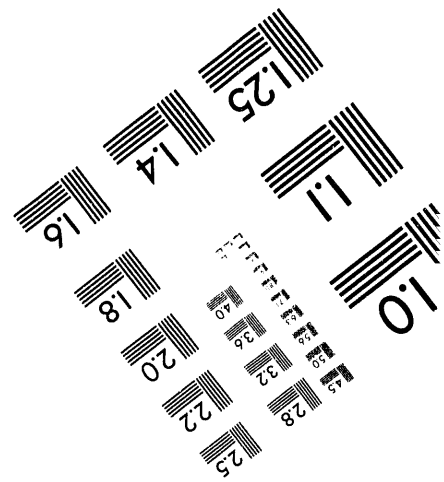

MANUFACTURED TO AIIM STANDARDS
BY APPLIED IMAGE, INC.

1 of 1

12/
8-11-94 JSO (1)

UCRL-ID-117079

A High Average Power Electro-Optic Switch Using KTP

C. A. Ebbers, W. M. Cook, and S. P. Velsko

April 1994

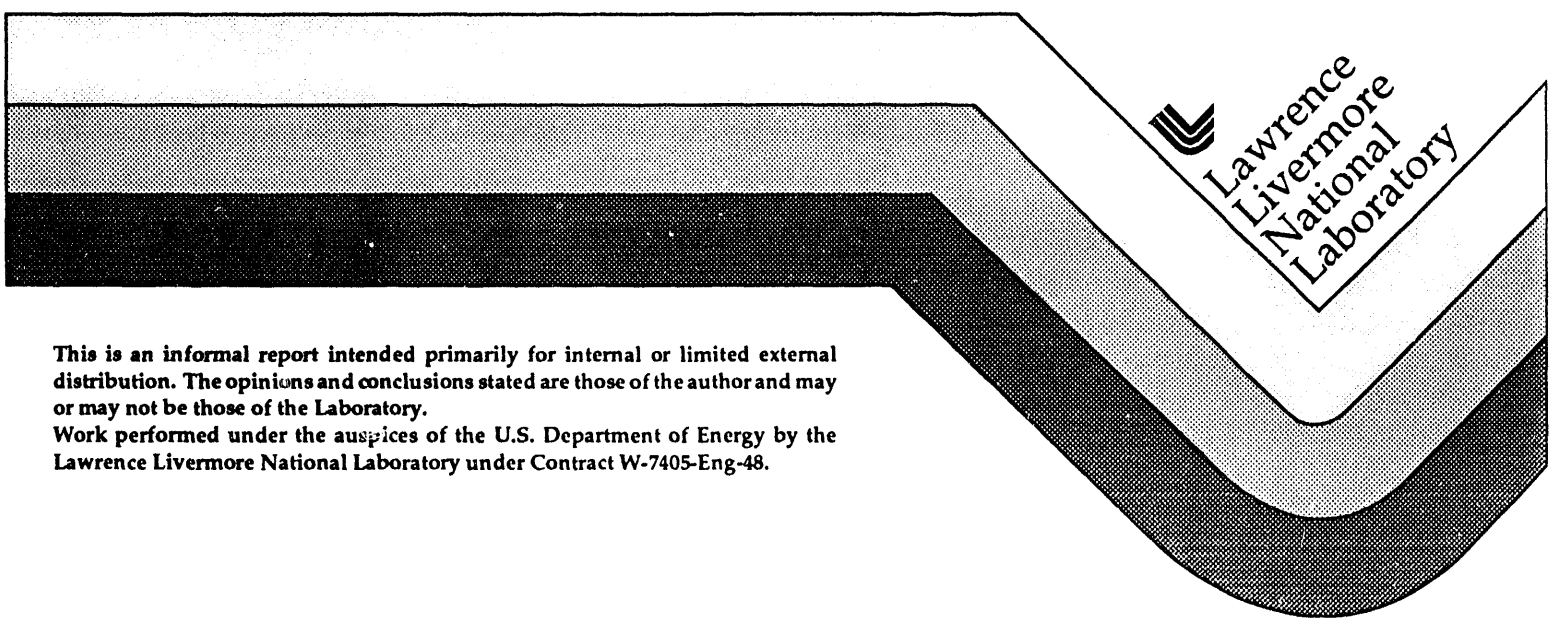

This is an informal report intended primarily for internal or limited external distribution. The opinions and conclusions stated are those of the author and may or may not be those of the Laboratory.
Work performed under the auspices of the U.S. Department of Energy by the Lawrence Livermore National Laboratory under Contract W-7405-Eng-48.

MASTER

DISCLAIMER

This document was prepared as an account of work sponsored by an agency of the United States Government. Neither the United States Government nor the University of California nor any of their employees, makes any warranty, express or implied, or assumes any legal liability or responsibility for the accuracy, completeness, or usefulness of any information, apparatus, product, or process disclosed, or represents that its use would not infringe privately owned rights. Reference herein to any specific commercial product, process, or service by trade name, trademark, manufacturer, or otherwise, does not necessarily constitute or imply its endorsement, recommendation, or favoring by the United States Government or the University of California. The views and opinions of authors expressed herein do not necessarily state or reflect those of the United States Government or the University of California, and shall not be used for advertising or product endorsement purposes.

This report has been reproduced
directly from the best available copy.

Available to DOE and DOE contractors from the
Office of Scientific and Technical Information
P.O. Box 62, Oak Ridge, TN 37831
Prices available from (615) 576-8401, FTS 626-8401

Available to the public from the
National Technical Information Service
U.S. Department of Commerce
5285 Port Royal Rd.,
Springfield, VA 22161

A High Average Power Electro-Optic Switch Using KTP

Christopher A. Ebbers, William M. Cook, and Stephan P. Velsko
Lawrence Livermore National Laboratory
P.O. Box 808, Livermore, CA 94550

Summary

High damage threshold, high thermal conductivity, and small thermo-optic coefficients make $KTiOPO_4$ (KTP) an attractive material for use in a high average power Q-switch. However, electro-chromic damage and refractive index homogeneity have prevented the utilization of KTP in such a device in the past. Our work shows that electro-chromic damage is effectively suppressed using capacitive coupling, and a KTP crystal can be Q-switched for 1.5×10^9 shots without any detectable electro-chromic damage. In addition, KTP with the high uniformity and large aperture size needed for a KTP electro-optic Q-switch can be obtained from flux crystals grown at constant temperature. A thermally compensated, dual crystal KTP Q-switch, which successfully produced 50 mJ pulses with a pulse width of 8 ns (FWHM), has been constructed. In addition, in off-line testing the Q-switch showed less than 7% depolarization at an average power loading of 3.2 kW/cm^2.

1. Background

There are essentially only three materials available for use as average power electro-optic switches for 1 μm solid state lasers: KD_2HPO_4 (DKDP), $LiNbO_3$, and $KTiOPO_4$ (KTP). All of these materials have low optical absorption at 1 micron and have large effective electro-optic coefficients. The other relevant merits and weaknesses of each material is displayed in Table I. DKDP has a low thermal conductivity which limits its utility as a transverse average power electro-optic modulator with a reasonable aspect ratio. Also, the only proven AR coating technology for DKDP are sol-gel coatings which limit the available clear aperture due to edge effects, and which tend to show a pronounced loss with age under normal handling conditions. $LiNbO_3$ has a much larger thermal conductivity but has a relatively low surface damage threshold. KTP has a combination of low optical absorption, high thermal conductivity, the ability to take "hard" AR coatings, and a damage threshold much higher than that of $LiNbO_3$. In addition, KTP does not display the prominent pyro-electric effect seen in $LiNbO_3$.

Using a thermally compensated $LiNbO_3$ electro-optic modulator, we recently demonstrated 250 watts of Q-switched average power ($\tau \sim 25$ ns).[1] However, it seems likely that the low surface damage threshold of $LiNbO_3$ will become problematic as we approach 1 kW or greater of Q-switched average power, given the multimode nature of the slab laser and its known beam nonuniformity. In addition, $LiNbO_3$ is a less compelling solution for slightly lower repetition rate (~ 500 Hz), higher pulse

energy (~ 1-2 J) lasers which are of interest for many applications. The prominent acousto-optic effect in $LiNbO_3$ also complicates cavity dumping schemes for short (~ 5 ns) pulse generation. Thus, we have investigated a thermally compensated, dual crystal Q-switch using KTP.

Table I. Comparative properties of DKDP, $LiNbO_3$, and KTP

Material	Damage threshold (J/cm^2)†	Thermal conductivity (mW/cm °K)	AR surface loss (per surface)	Acoustic-optic effect	Applied field damage effects
DKDP	> 50	12 (o), 15 (e)	high†††	small	electro-migration
$LiNbO_3$	1-4	45 (o), 41 (e)	< 0.25%	large	none
KTP	> 15	~40††	< 0.25%	small	electro-chromic

† $\lambda = 1.06\ \mu m$, $\tau = 10$ ns

†† estimate

††† edge effects and scatter

Two problems hinder the direct application of KTP in an electro-optic switch: the electro-chromic effect and optical inhomogeneity. A description of the electro-chromic effect and its solution is presented in Section 2. We have also observed that static strain depolarization is a problem in KTP, unlike in DKDP and Z axis $LiNbO_3$. This problem must be solved in pieces of specific aperture and length, determined in Section 3. In Section 4 the measured depolarization of KTP crystals obtained from several vendors/growth techniques is compared. The strain depolarization problem is circumvented by requiring that the pieces be obtained from single growth sectors of crystals grown at constant temperature. At least one vendor can provide such material of the required volume. The tolerances of a dual crystal, thermally compensated KTP Q-switch are discussed in Section 5. Finally, Section 6 contains a description of the test results of a KTP Q-switch constructed from a large aperture, optically homogeneous KTP crystal.

2. Electro-Chromic Damage

KTP is a potassium super-ionic conductor (the ionic conductivity in KTP is much higher than in typical dielectrics). In addition, KTP also exhibits an electro-chromic effect.[2] Electrons injected at the anode of the crystal can reduce the stoichiometric Ti^{4+} ions in the crystal lattice to Ti^{3+}. Upon application of an electric field, a black absorbing band moves from the anode towards the cathode in the crystal of KTP, compromising its utility as a Q-switch. The rate of this black band migration is correlated with the magnitude of conductivity of the KTP and can be quite rapid. One 5 x 5 x 5 mm^3 crystal we obtained was entirely blackened after 90 seconds with an applied field of 1.3 kV/cm. Figure 1 shows the electro-chromic damage present in another crystal after 4 hours under similar conditions.

The electro-chromic damage rate is dependent upon the conductivity of the individual KTP crystal, and can vary significantly ($\sigma \sim 1 \times 10^{-06} - 1 \times 10^{-09}$ S/cm) depending upon the growth technique. In general, the conductivity of high temperature solvent grown crystals is greater than that of hydrothermally grown

crystals. The conductivity can be significantly lowered through the incorporation of trivalent dopants (Ga^{3+}, Sc^{3+}, etc.) into the KTP crystal lattice ($\sigma_{flux} > \sigma_{hydrothermal} > \sigma_{doped}$). By using a low conductivity crystal, the electro-chromic damage rate can be minimized. However, large aperture hydrothermal KTP is not yet available, and doped KTP shows significant variations in the birefringence across the aperture, due to differential incorporation of the dopant ions. Using 1 mil thick sheets of acetate to block the flow of current, it was observed that simply applying an electric field across a high conductivity flux grown KTP crystal was not sufficient to induce electro-chromic damage in the sample, that is, there must be a transport of charge into the material as opposed to simply inducing an internal rearrangement of ions in the crystal. Thus, by inserting a blocking capacitor in series with the crystal, electro-chromic damage in the crystal can be avoided.

The equivalent circuit is shown in Figure 2. The external capacitance and crystal capacitance act as a voltage divider network, and the effective resistance of the crystal determines the discharge time of C_B. Choosing $C_B \sim 1{,}000$ pf and with the typical values of $R_{cryst} \sim 10\text{-}100$ MΩ, the time constant of this differentiator is ~ 0.1-1 second, sufficient enough time to allow Q-switching to occur. To the right of Figure 2, the differentiation characteristic of the voltage across the crystal is seen for long pulse durations. However, on the 200 ns timescale, the voltage across the electro-optic crystal is essentially constant. With the typical value of $C_{cryst} \sim 10\text{-}20$ pf, greater than 99% of the voltage drop is across C_{cryst}. The rise-time of the circuit in Figure 2 is dependent upon the inductance in the circuit, a function of electrical lead length (estimated lead self-inductances of ~ 0.004 μH/mm have not been included in the above model).

By using a capacitively coupled circuit, a 6 x 6 mm^2 aperture KTP crystal, 9 mm in length has been Q-switched repetitively (1.5×10^9 shots, 1 week, 2,500 Hz, 3,000 volts) without the formation of electro-chromic damage (as observed by eye and spectro-photometrically). Periodically the voltage was checked to ensure that indeed the half-wave voltage was being applied. This crystal has been Q-switched under all available voltage configurations; a negative going dual ended pulse, a single ended negative pulse, and a dual ended positive going pulse (available using a Krytron switch, a single Thyratron switch, and MOSFET pulse drivers). One advantage of KTP over $LiNBO_3$ is immediately apparent in Figure 3, showing the optical response of a pulsed $LiNbO_3$ crystal vs. the optical response of a KTP crystal. The acousto-optic effect in KTP is significantly reduced compared to $LiNbO_3$, resulting in a fast optical switch off and eliminating the need for a bias voltage to drive the switch off. KTP thus has a significant advantage over $LiNbO_3$ for cavity dumping applications, where the switch must remain in the on condition for up to a microsecond, but then must abruptly turn "off."

3. Dimensions of the KTP Q-Switch Crystals

Figure 4 shows the arrangement of a pair of KTP crystals in a thermally compensated arrangement. In an ideal pair of crystals, the birefringence, thermally induced birefringence, and the stress-optic induced depolarization would vanish. When the ideal crystal arrangement of Figure 4 is placed between parallel polarizers,

no light would be transmitted across the aperture. If a 90° rotator is placed after the compensated crystal pair, again between parallel polarizers, the maximum intensity is transmitted. We are interested in measuring the fraction of light which is depolarized due to uncompensated birefringence. The depolarization fraction is determined from the expression:

$$I_{depolarization} = I_{rotator\ removed} / (I_{rotator\ removed} + I_{rotator\ inserted})$$

The input aperture (20 x 7 mm^2 for the kilowatt slab laser and 7 x 7 mm^2 for the ATDR laser) and maximum convenient switching voltage (2.4 kV) sets a limit on the minimum crystal volume needed for the thermally compensated Q-switch as shown in Figure 4. There are five potentially useful configurations, displayed in Table II; Z propagation, X propagation or Y propagation, with the Z crystallographic axis normal or rotated 45° with respect to the applied electric field.

Table II. Length specification for bicrystal KTP Q-switch

(λ = 1.06 μm, V_π = 2.4 kV, width = 0.7 cm)

k (propagation direction)	(θ,ϕ,ψ) cut specification	r_{eff} (pm/V) effective EO coefficient	Crystal length (cm)	Total (2 pass) propagation thickness (cm)
Z (Vπ = 31 kV)	(0,-,0)	33.8	independent	independent
X	(90, 0, 0)	138.6	0.56	2.24
X (YZ rotated)	(90, 0, 45)	98.0	0.79	3.16
Y	(90, 90, 0)	172.4	0.45	1.80
Y (XZ rotated)	(90, 90, 45)	121.9	0.64	2.55

The non-rotated cuts require an additional pair of 45° rotators to be inserted around the crystal pair. It is generally desirable to minimize the number of elements in the optical train and to minimize the total crystal length, making the last entry in Table II the preferred crystal orientation. However, the growth method and external habit of a KTP crystal will determine the maximum volume of high quality KTP available from that crystal with a particular orientation, which may necessitate the use of a less desirable cut.

4. Birefringence Variations in KTP

To achieve a depolarization loss of less than 10%, the birefringence across the aperture of the two crystals shown in Figure 4 must be constant to within ~1 ppm across the longest dimension of the desired aperture. Unfortunately, the birefringence of flux or hydrothermally grown KTP does not typically fall within this tolerance. Care must be taken to select the desired crystals from areas which yield the highest quality material, which is dependent upon the growth method. Figure 5 shows the light transmitted through a pair KTP crystals (at room temperature) in the compensated arrangement of Figure 4. The false color scale is set such that blue (or black) represents a minimum in transmitted intensity, while red (or white) represents the maximum in transmitted intensity. We measured an

aperture integrated depolarization loss fraction near 50%, as evidenced by the maximum and minimum transmitted intensity variations across the aperture. The optical quality of the surface finish of the crystals was confirmed to be $\lambda/20$, with a parallelism of 5", ensuring that it was an internal, inhomogeneous strain that we were measuring, versus the effect of a wedge or surface finish problem. The crystals used are 7.25 x 7.25 x 8 mm^3, grown using the temperature drop flux method. A series of four crystals were available and these are the best pair. To the best of our knowledge, these crystals represented the "state-of-the-art" in large aperture, flux grown KTP obtainable within the last year.

Static depolarization measurements on nine other flux and hydrothermally grown KTP crystals show a consistent pattern: all of the temperature drop flux grown crystals we have examined show high depolarization losses. In contrast, of the four high temperature hydrothermally grown KTP crystals we have examined, two 5 x 5 x 5 mm^3 and two 5 x 5 x 10 mm^3, three crystals had significantly lower losses than the flux grown crystals and the fourth had an equivalent loss. However, hydrothermally grown KTP is currently limited to apertures of approximately 7 x 7 mm^3. A new lower temperature hydrothermal growth process may eventually produce KTP of the required aperture, but larger aperture hydrothermally grown KTP crystals are currently unavailable.

Recent work[3] has shown that in the case of a top seeded "K6 flux" grown KTP crystal, the change in birefringence is predominantly due to the change in the n_z index and is directly related to the monotonically decreasing temperature to which the crystal is subjected to during the growth process. This was determined by measuring the change in the phasematching angle across a single crystal slice of KTP, 50 x 25 mm^2 in aperture. The measured phasematching angle as a function of position roughly followed a quadratic profile from edge to edge of the slice, varying by 0.5° from center to edge. Using polarized interferometry the variation in the n_z index was shown to be two orders of magnitude larger than the variation in the n_{xy} index. This allows an estimate of the changing n_z index to be placed at 6.4×10^{-4}/cm. The precise variation (linear, quadratic, etc.) of n_z with temperature (correlated with position) could not be determined due to scatter in the phasematching data. Although the flux grown KTP crystals we examined were probably grown using different temperature profiles than the crystal above, a straightforward model shows that the aperture integrated depolarization loss measurements we made are consistent with this value of the change in birefringence. In addition, modeling shows that to obtain low loss-large aperture crystals, the change in birefringence per centimeter of aperture needs to roughly be a factor of five smaller than that of the flux grown crystals we have already examined. Two factors may contribute to the lower depolarization losses observed in hydrothermally grown KTP. The crystals are grown using [101] seeds, thus the crystals obtained from each boule are cut from nearly "single growth sector" material. In addition, the crystals are grown using a near constant temperature approach; a fixed thermal gradient and convection supply the supersaturated solute needed for crystal growth.

Figure 6 shows a picture of a large aperture flux grown KTP crystal obtained from Hoya grown using a new constant temperature growth technique.[4] In addition to

the potential benefit of growth at constant temperature, the external habit is such that large aperture, single growth sector crystals can be obtained. Figure 7 shows a picture of the crystals obtained after cutting, 8 x 11 x 16 mm^3 along X, Y, and Z respectively. In Figure 8a, the transmitted wavefront of "best" of the four 7.25 x 7.25 mm^2 is shown in comparison with the transmitted wavefront of one of the crystals obtained from Hoya in Figure 8b. The fine horizontal fringes seen in both crystals are due to the parallelism of the front and back surfaces. While slight internal strain is seen in the crystal from Hoya, especially near the region from which the seed is cut (on the right), significantly more internal index inhomogeneity is observed in the smaller aperture, temperature drop grown crystal. Depolarization loss measurements also confirm the higher optical quality of the crystal from Hoya. The aperture integrated depolarization measured across a 1 cm diameter aperture was 4.1% in the crystals grown by the constant temperature growth technique, shown in Figure 9. This is in contrast to the 48% depolarization measured in the 7.25 mm diameter aperture, temperature drop grown KTP of Figure 5. This is a single pass loss measured at 632.8 nm. The thickness of the constant temperature grown KTP crystal pair is 16.8 mm. The thickness of the temperature drop grown KTP crystal pair is 16 mm. The refractive index inhomogeneity present in the constant temperature grown crystals is significantly less than in other flux grown KTP crystals with 1/2 the aperture and is comparable to the best obtained from the hydrothermally grown KTP with 1/6 the aperture of the Hoya KTP.

5. Dimensional and Angular Tolerances of a KTP Q-Switch Assembly

The minimum acceptable depolarization loss from all sources (static strain, alignment, fabrication tolerances, and thermal strains) is dependent upon the gain present in the particular laser cavity: lower gain cavities can withstand higher static depolarization losses. For the slab laser (a low gain system), it is desired to hold the total depolarization loss from all sources to less than 10%. For the ATDR laser (a high gain cavity) it is assumed that the total depolarization loss cannot exceed 2%. Of the various ways of incurring a depolarization loss, nonuniform birefringence, nonuniform thickness, differing path lengths between crystals, or misorientation of one crystal relative to the other, it is assumed that the controllable depolarization loss (controllable through fabrication tolerances) should be kept to within 0.1% maximum each item for both the slab laser and the ATDR laser. Table III contains the dimensional and angular tolerances needed to maintain the 0.1% depolarization loss. While rigorous, these tolerances are not beyond the capabilities of existing suppliers or fabricators. It should be noted that an additional $\lambda/4$ waveplate is necessary for normal operation of this finite birefringence switch. This additional waveplate could be eliminated if one crystal could be precisely polished to act as quarter wave retarder. Unfortunately, a precision removal of the approximate (2n)*2.5 microns of material across the aperture of one crystal while maintaining the parallelism of the faces is extremely difficult.

Table III. Sensitivity of static birefringence compensation extrinsic to the crystal (λ = 1.06 μm, V_π = 2.4 kV, width = 0.7 cm, Length = 2.55 cm)	
Type of fabrication variation	Maximum tolerance (< 0.1% depolarization @ 1.064 microns)
Relative differential propagation length of crystal 1 with respect to (WRT) crystal 2	0.5 microns (λ/2)
Wedge of crystal 1 or 2 across 2 cm aperture	10″
Wedge of crystal 1 or 2 across 0.7 cm aperture	11″
Rot. of X-Z plane of crystal 2 WRT crystal 1	600″
Rot. in Y-Z plane of crystal 2 WRT crystal 1	600″
Rot. in X-Y plane of crystal 2 WRT crystal 1	2000″

6. Performance of a KTP Q-Switch Assembly

Two 8.23(X) x 10.54(Y) x 6.94(Z) mm^3 crystals were obtained from one of the 8 x 11 x 16 mm^3 crystals described in Section 4. These crystals and 90° rotator were thermally bonded to a ceramic substrate. The propagation direction was parallel to the X axis, and the Z faces were parallel to the substrate. Two 6 kV blocking capacitors of 0.02 μf were wired in series and mounted on the assembly, shown in Figure 10. The depolarization loss measured for this Q-switch at 632.8 and 1064 nm was 1.76% and 0.625% (contrast ratios of 1:55 and 1:158), respectively, over the entire 10.54 x 6.94 mm^2 aperture. These values are in very good agreement with the modeled wavelength dependence of the depolarization loss. The total insertion loss (due to scatter, optical absorption, and the predominant reflection losses) of the KTP Pockels cell was measured to be 2.5%. This value is not unreasonable given that dual-wavelength AR coatings (632, 1064 nm) were used on the KTP crystals. However, the optimized loss for this device will probably not be lower than 1.5% given the typical loss value of 0.25%/surface for a standard single wavelength AR coating.

Q-switching of this device was demonstrated in the "γ-lidar" laser; a compact, end-pumped Nd^{3+}:YLF laser oscillator similar to that described in Reference 5, with the significant difference in that this oscillator is pumped by ~ 70 air-cooled diode bars, limiting the pulse repetition rate to 1 Hz and the average power to approximately 0.1 watts. The optical setup is shown in Figure 11. Two different cavity lengths were tested. A summary of the output power, pulse width, and depolarization loss due to the insertion of the KTP Pockels cell is shown in Table IV. The difference in CW output power between the bare cavity setup and the Q-switched cavity setup was due to the additional reflection losses of the KTP Q-switch and λ/4 waveplate in addition to the finite aperture (6.95 mm vs 8 mm) of the KTP Q-switch. No attempt was made to optimize the output coupler for the Q-switched cavity. The optimal Q-switch voltage was experimentally determined by measuring the output power as a function of applied Q-switch voltage, displayed in Figure 12. The optimal voltage was found to be 1.6 kV, in good agreement with the published

electro-optic coefficients.[6] Overall, the laser was Q-switched for ~10 hours (36,000 shots) without detectable damage of the optical surfaces. The maximum Q-switched output observed was 52 mj in an 8 ns pulse.

Table IV. Q-switched output power obtained using the KTP compensated Q-switch

Cavity length (optical)	CW Bare cavity output power (mJ)	QS output power (mJ)	CW output power (mJ)	QS Pulse width (ns, FWHM)	Depolarization (output)
40.0 cm	53.3	31.2	37.25	17.00 ns	1.08%
27.5 cm	73.0	40.3	48.50	8.25 ns	1.13%

The thermal compensation of the KTP Q-switch was tested off-line, using a high average power welding laser as a substitute for the thermal load. This apparatus is described in detail in Reference 7. The small aperture (6.9 x 11 mm^2) of the KTP Q-switch necessitated the off-line testing, as the average power slab lasers at LLNL currently require a 7 x 20 mm^2 aperture. In summary, the device under test is place into the cavity of a Quantronix 118 welding laser. Dichroic mirrors allow the probing of the thermo-optic effects using a well polarized 632.8 nm light with a flat-top spatial profile. The depolarization ratio is determined as in Section 3. The depolarization loss as a function of thermal loading is shown in Figure 13. The depolarization loss is dependent upon the wavelength that the measurement is performed. For small losses (< 15%), the following equation is valid:

$$\%\text{Depol}(\lambda 2) = \%\text{Depol}(\lambda 1) * (\lambda 2/\lambda 1)^2$$

The depolarization loss at 1.064 μm is also shown in Figure 13. It is seen that at an average power loading of 3.2 kW/cm^2 the aperture integrated depolarization loss at 1.064 μm is less than 7%. The equivalent uncompensated switch shows 50% depolarization above 500 W/cm^2.

References

1. S. P. Velsko, C. A. Ebbers, B. Comaskey, G. F. Albrecht, S. C. Mitchell, "100 Watt Average Power at 0.53 μm by External Frequency Conversion of an Electro-Optically Q-Switched Diode Pumped Power Oscillator," submitted to Applied Physics Letters (Dec. 1993).
2. V. V. Lemeshko, V. V. Obukhovskii, A. V. Stoyanov, N. I. Pavlova, A. I. Pisanskii, and P. A. Korotkov, "Electro-Chromic Effect in Potassium Titanate-Phosphate Crystalsk," Ukrainskii Fizicheskii Zhurnal, **31**, pp. 1746-1750 (1986).
3. T. Sasaki, A. Miyamoto, A. Yokotani, and S. Nakai, "Growth and Optical Characterization of Large Potassium Titanyl Phosphate Crystals," ICCG-10, August 16, 1992, San Diego, CA.
4. K. Sato, K. Okada, and Y. Toratani, "A Constant Temperature Growth of Sector Boundary-Free KTP," The 40th Spring Meeting of the Japan Society of Applied Physics, March 1993, Tokyo, Japan.

5. R. Beach, P. Reichert, W. Benett, B. Freitas, S. Mitchell, S. Velsko, J. Davin, and R. Solarz, "Scalable Diode-End-Pumping Technology Applied to a 100 mJ Q-Switched Nd^{3+}:YLF Laser Oscillator," Opt. Lett. **18**, pp. 1326-1328 (1993).
6. J. D. Bierlein and C. B. Arweiler, "Electro-Optic and Dielectric Properties of $KTiOPO_4$," Appl. Phys. Lett. **49**, pp. 917-919 (1986).
7. S. P. Velsko and C. A. Ebbers, "High Average Power Q-Switch Design," in preparation.

Figure 1. Electro-chromic damage present after 4 hours @ 1200 V/cm in CTI crystal.

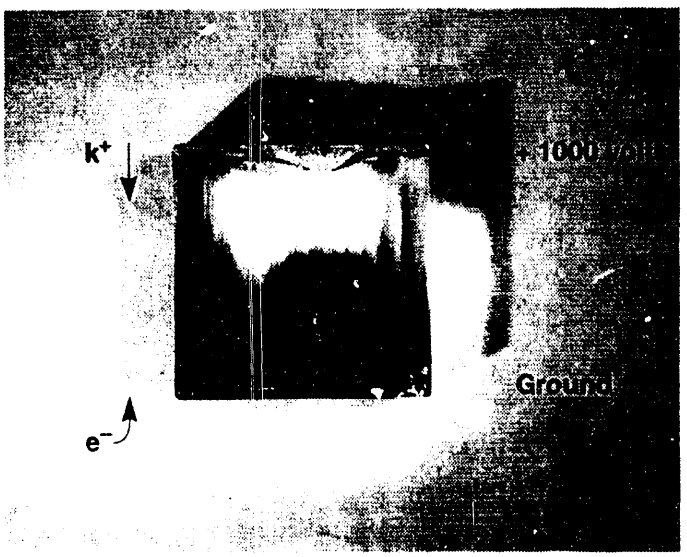

99-00-1293-4373.pub

Figure 2. Equivalent circuit for capacitively coupled circuit.

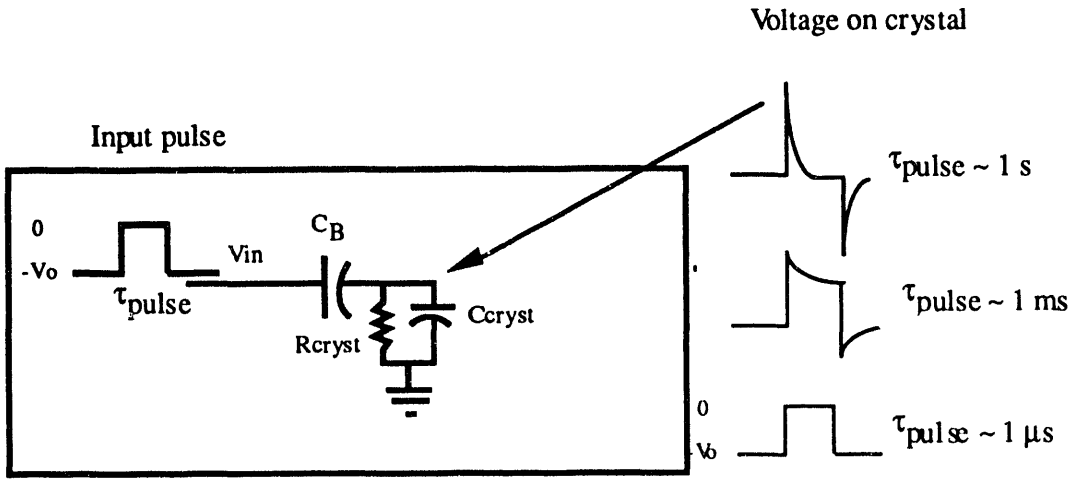

Figure 3. (a) Long pulse optical response of $LiNbO_3$ to voltage pulse.
(b) Long pulse optical response of KTP to voltage pulse.

(a)

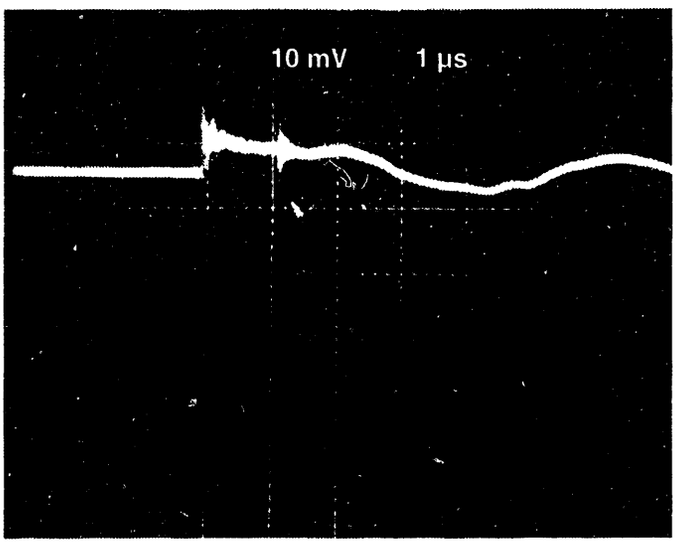

99-00-1293-4371.pub

(b)

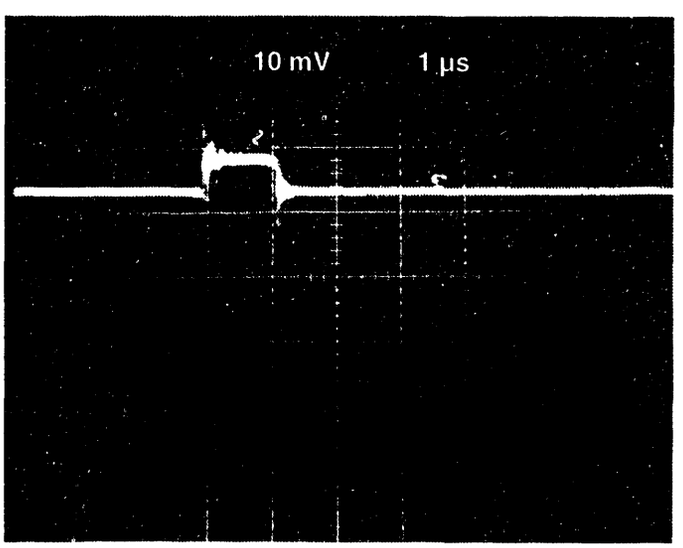

99-00-1293-4372.pub

Figure 4. Transverse, bicrystal, thermally compensated switch.

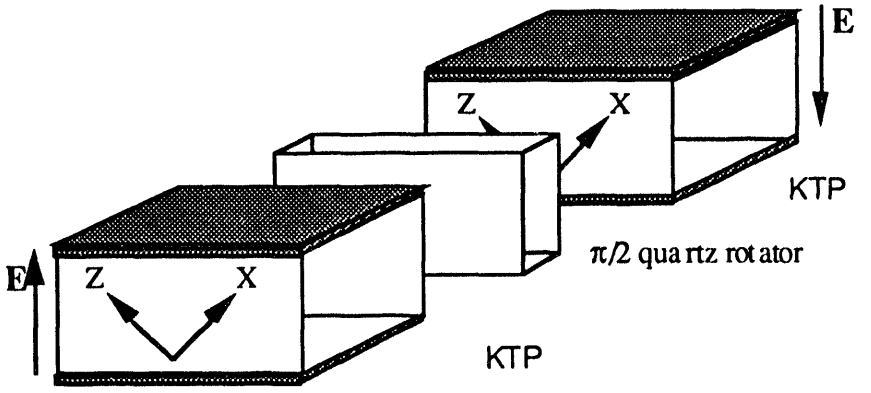

Figure 5. Depolarization of 7.25x7.25x8 mm^3 pair of CSK flux growth KTP crystals.

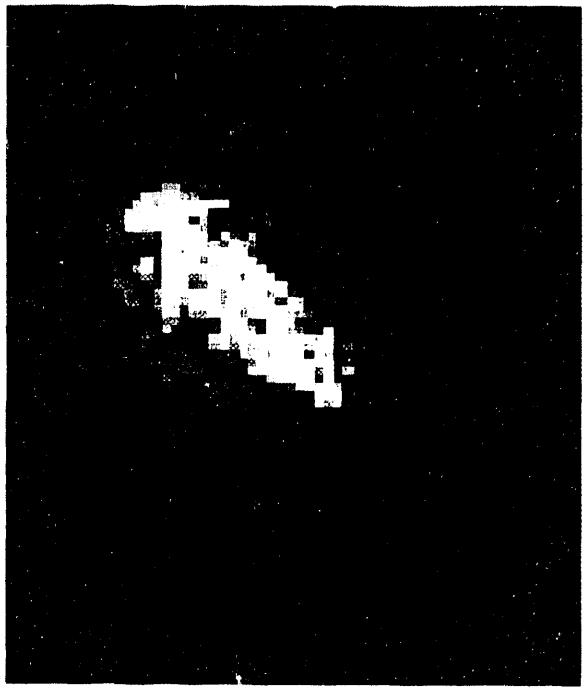

Figure 6. Hoya, 18x25x27 mm^3 KTP crystal grown using constant temperature flux growth technique.

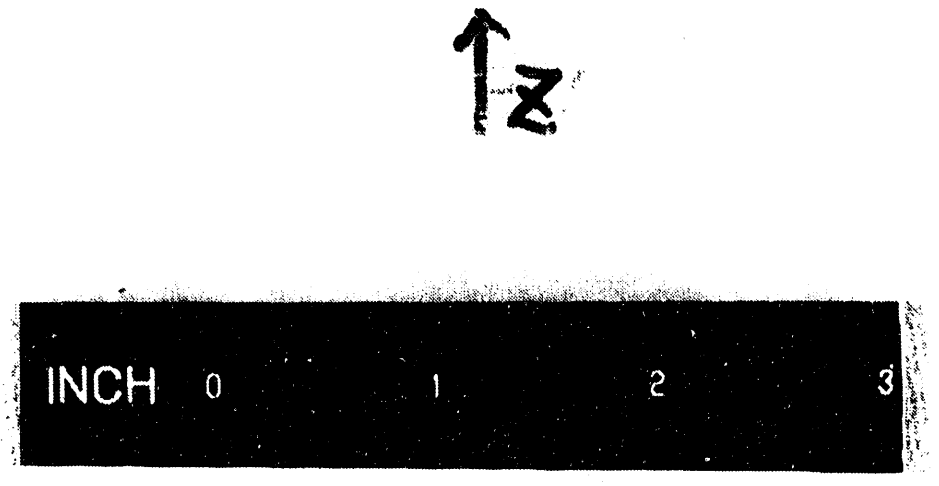

Figure 7. Single growth sector, 8x11x16 mm^3 crystals cut from Hoya boule.

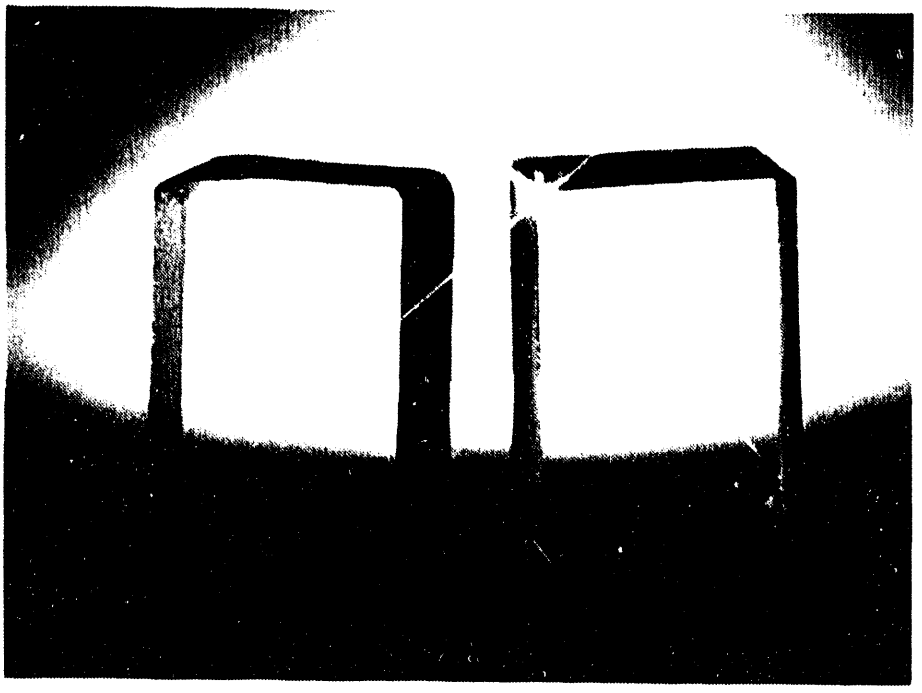

Figure 8. (a) Transmitted wavefront of 7.25x7.25x8 mm^2 CSK crystal.
(b) Transmitted wavefront of 8x11x16 mm^3 Hoya crystal.

(a)

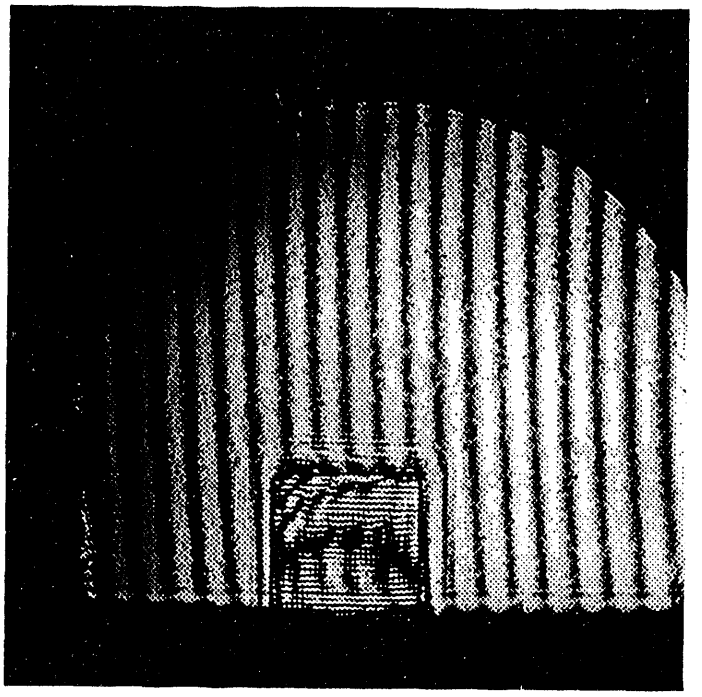

(b)

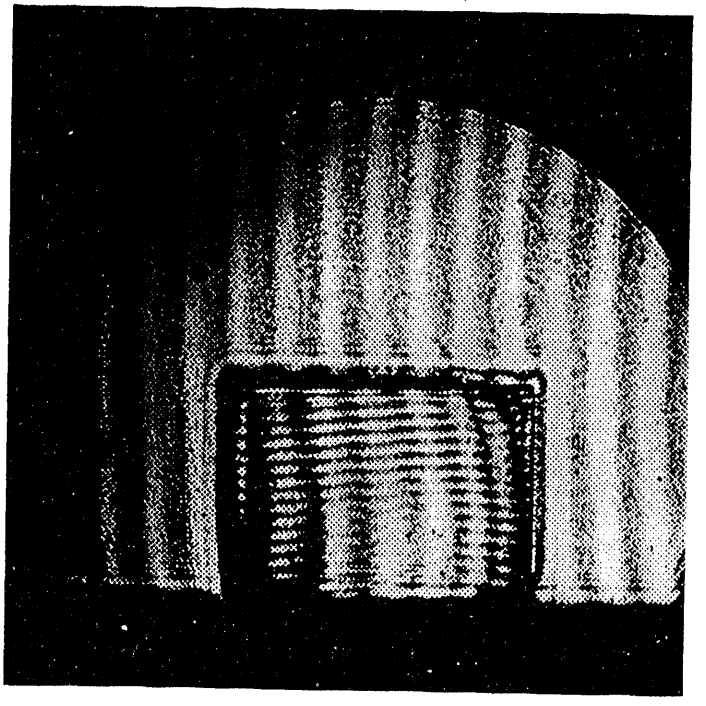

Figure 9. Depolarization of 11x15x8.4 mm^3 pair of Hoya constant temperature grown KTP crystals.

Figure 10. KTP Q-switch assembly.

Figure 11. Q-switch test setup.

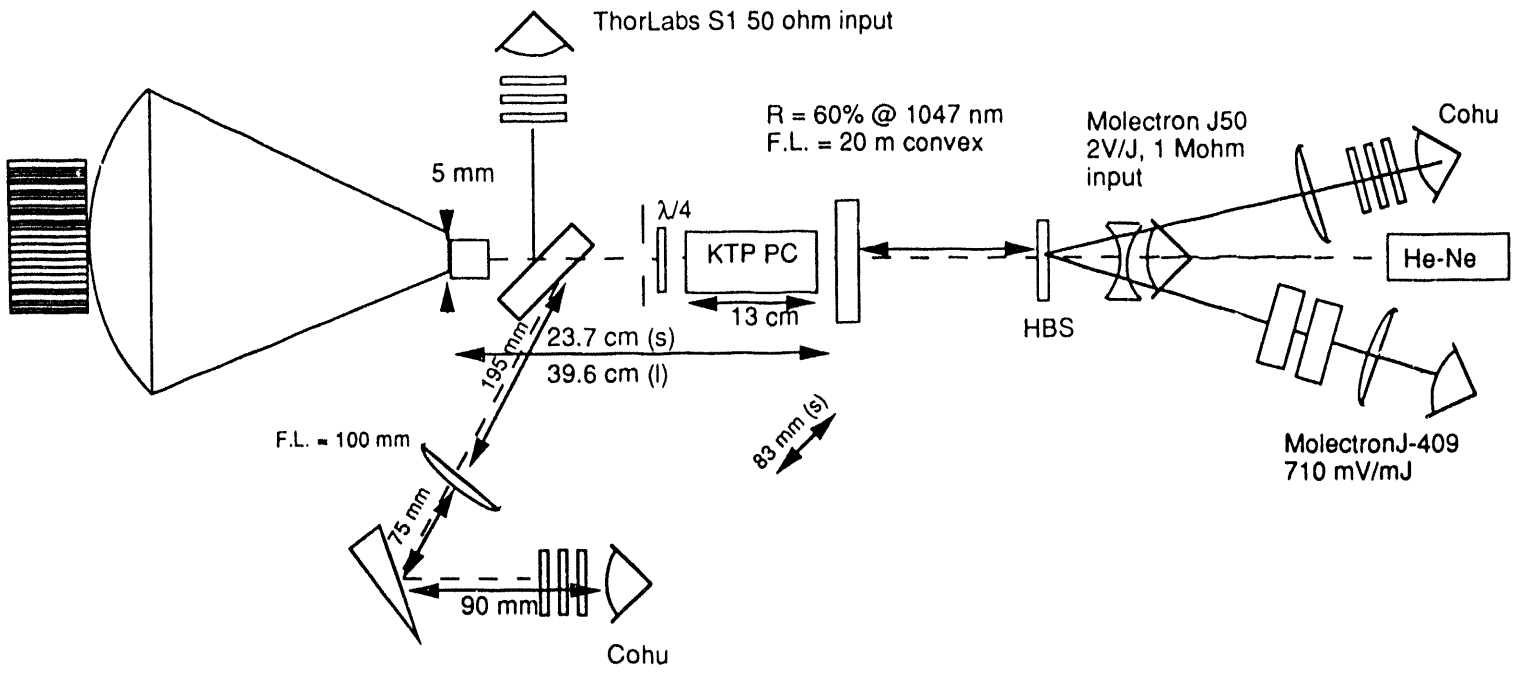

Figure 12. The quarter-wave voltage for the compensated KTP Q-switch was 1.6 kV.

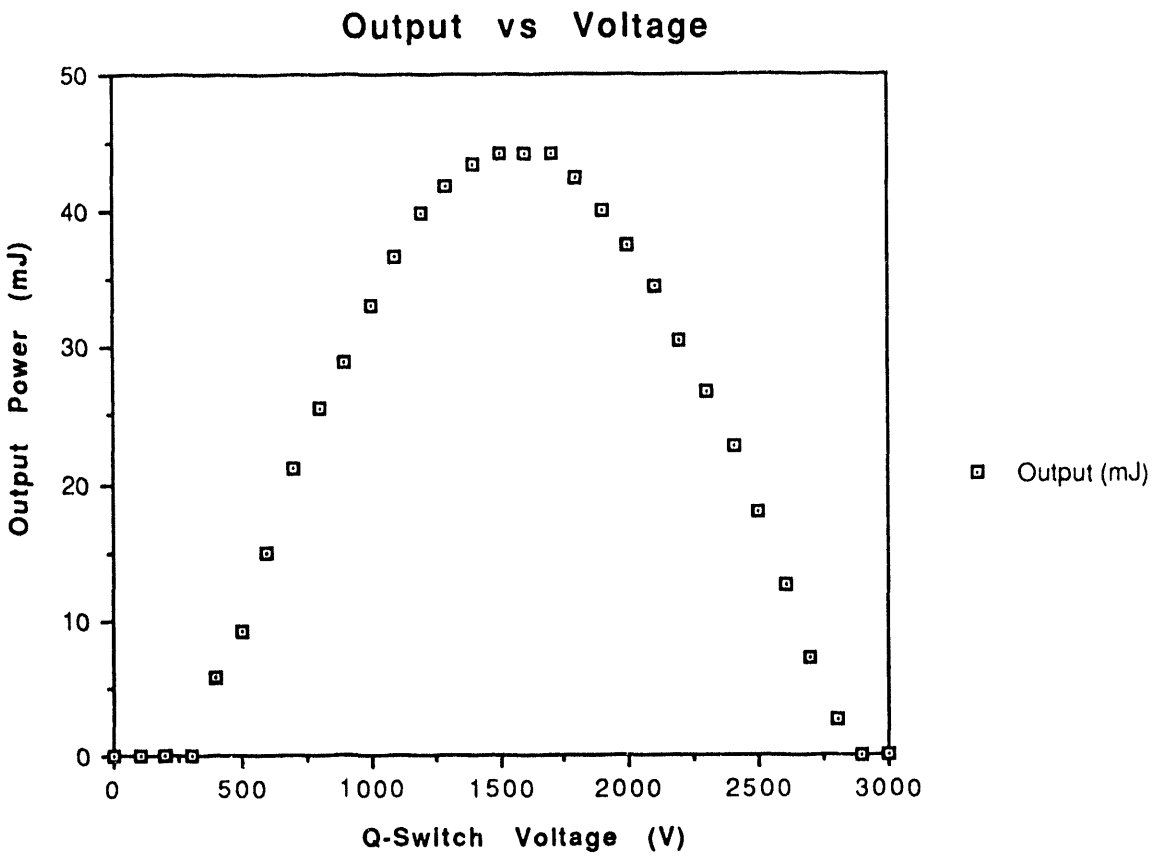

Figure 13. Measured depolarization loss in the compensated KTP Q-switch. (Measured at 632 nm and calculated for 1.064 μm).

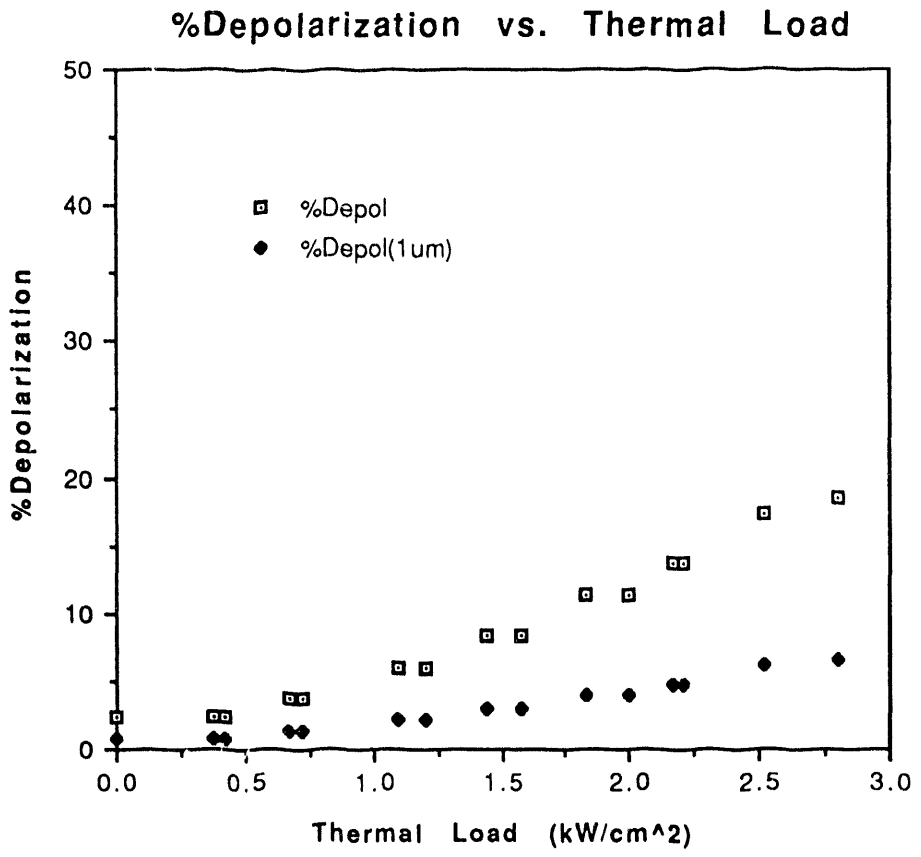

DATE FILMED

9/8/94

END